Inorg. Chem. **2008**, *47*, 3486−3488

Assessment of the Anisotropy in the Molecule Mn_{19} with a High-Spin Ground State $S = {}^{83}/_{2}$ by 35 GHz Electron Paramagnetic Resonance

Oliver Waldmann,*,† Ayuk M. Ako,‡ Hans U. Güdel,§ and Annie K. Powell‡

Physikalisches Institut, Universität Freiburg, D-79104 Freiburg, Germany, Institut für Anorganische Chemie, Universität Karlsruhe, D-76128 Karlsruhe, Germany, and Department für Chemie and Biochemie, Universität Bern, CH-3012 Bern, Switzerland

Received February 1, 2008

35 GHz electron paramagnetic resonance experiments on a powder sample of the magnetic molecule Mn_{19} with a high-spin ground state $S = {}^{83}/_{2}$ are presented. At low temperatures, the data are well described by the simulated spectra for an isolated spin with a zero-field-splitting parameter $D = 0.004$ cm^{-1}, which is, in particular, positive. Hence, Mn_{19} is not a single-molecule magnet; the previously observed magnetic hysteresis at ultralow temperatures is likely due to intermolecular dipolar interactions.

The discovery of slow relaxation of the magnetization in the high-spin molecule $[Mn_{12}O_{12}(CH_3COO)_{16}(H_2O)_4]\cdot 2CH_3COOH\cdot 4H_2O$ (Mn_{12} acetate) more than a decade ago has inspired a flurry of research activities, in both chemistry and physics.[1] In these now so-called single-molecule magnets (SMMs), the time scale of the magnetic relaxation may become very long at temperatures below a blocking temperature T_B, such that each molecule, in principle, may function as a data-storage unit. However, in Mn_{12} acetate, $T_B = 3.5$ K, which is too small for applications, and raising T_B is an important goal. The blocking temperature is related to an anisotropy barrier $\Delta = DS^2$, where S is the molecular ground-state spin and D the uniaxial magnetic anisotropy parameter (which has to be of the easy axis type, $D < 0$). In the hope of being able to raise T_B to higher levels, much effort has been devoted to the synthesis of new molecules with ever higher ground-state spin S (it, however, recently became clear that larger S, in general, does not imply larger barriers or blocking temperatures[3]).[2]

The largest spin to date, $S = {}^{83}/_{2}$, was very recently achieved in the compound $[Mn_{19}O_8(N_3)_8(HL)_{12}(MeCN)_6]Cl_2\cdot 10MeOH\cdot MeCN$ [H_3L = 2,6-bis(hydroxymethyl)-4-methylphenol], or Mn_{19} for short.[4] The 12 Mn^{III} ions (spin 2) and 7 Mn^{II} ions (spin $^5/_2$) are ferromagnetically coupled, giving rise to the high-spin ground state ($S = 12 \times 2 + 7 \times {}^5/_2 = {}^{83}/_2$). Although the Mn^{III} ion is well-known for significant easy-axis anisotropies, due to the Jahn−Teller effect, and in spite of the huge ground-state spin, Mn_{19} does not exhibit a clear SMM behavior. The magnetization curve, in fact, was found at low temperatures to follow very closely the Brillouin function predicted for isolated $S = {}^{83}/_{2}$ spins with no anisotropy. Only at temperatures below 0.5 K was magnetic hysteresis observed, which it was suggested could be due to SMM behavior and/or intermolecular magnetic interactions.[4] Thus, in order to further understand the magnetism in Mn_{19}, it is clearly important to gain insight into the magnetic anisotropy. In this Communication, we present powder Q-band electron paramagnetic resonance (EPR) spectra at low temperatures, which show that $D = 0.004$ cm^{-1}. D is, in particular, positive. Hence Mn_{19} is not a SMM, and the observed magnetic hysteresis is assigned to intermolecular magnetic interactions.

A polycrystalline sample of Mn_{19} was synthesized following ref 4 The EPR spectra were recorded on a standard Q-band (34 GHz) Bruker EPR spectrometer. Temperature control was achieved via a ^{4}He cryostat; the lowest nominal temperature was 4 K, but the installed thermocouple sensor is not precise at these low temperatures. Two samples were measured: one that was prepared from the polycrystalline

* To whom correspondence should be addressed. E-mail: oliver.waldmann@physik.uni-freiburg.de.
† Universität Freiburg.
‡ Universität Karlsruhe.
§ Universität Bern.

(1) (a) Caneschi, A.; Gatteschi, D.; Sessoli, R.; Barra, A. L.; Bruel, L. C.; Guillot, M. *J. Am. Chem. Soc.* **1991**, *113*, 5873. (b) Sessoli, R.; Gatteschi, D.; Caneschi, A.; Novak, M. A. *Nature* **1993**, *365*, 141. (c) Christou, G.; Gatteschi, D.; Hendrickson, D. N.; Sessoli, R. *MRS Bull.* **2000**, *25*, 66. (d) Gatteschi, D; Sessoli, R. *Angew. Chem., Int. Ed.* **2003**, *42*, 268. (e) Bircher, R.; Chaboussant, G.; Dobe, C.; Güdel, H. U.; Ochsenbein, S. T.; Sieber, A.; Waldmann, O. *Adv. Funct. Mater.* **2006**, *16*, 209.

(2) (a) Heath, S. L.; Powell, A. K. *Angew. Chem., Int. Ed.* **1992**, *31*, 191. (b) Larinova, J.; Gross, M.; Pilkington, M.; Andres, H.; Stoeckli-Evans, H.; Güdel, H. U.; Decurtins, S. *Angew. Chem., Int. Ed.* **2000**, *39*, 1605. (c) Zhong, Z. J.; Seino, H.; Mizobe, Y.; Hidai, M.; Fujishima, A.; Ohkoshi, S. I.; Hashimoto, K. *J. Am. Chem. Soc.* **2000**, *122*, 2952. (d) Low, D. M.; Jones, L. F.; Bell, A.; Brechin, E. K.; Mallah, T.; Rivière, E.; Teat, S. J.; McInnes, E. J. L. *Angew. Chem., Int. Ed.* **2003**, *42*, 3781. (e) Murugesu, M.; Habrych, M.; Wernsdorfer, W.; Abboud, K. A.; Christou, G. *J. Am. Chem. Soc.* **2004**, *126*, 4766.

(3) Waldmann, O. *Inorg. Chem.* **2007**, *46*, 10035.

(4) Ako, A. M.; Hewitt, I. J.; Mereacre, V.; Clérac, R.; Wernsdorfer, W.; Anson, C. E.; Powell, A. *Angew. Chem., Int. Ed.* **2006**, *45*, 4926.

10.1021/ic800213w CCC: $40.75
Published on Web 04/05/2008

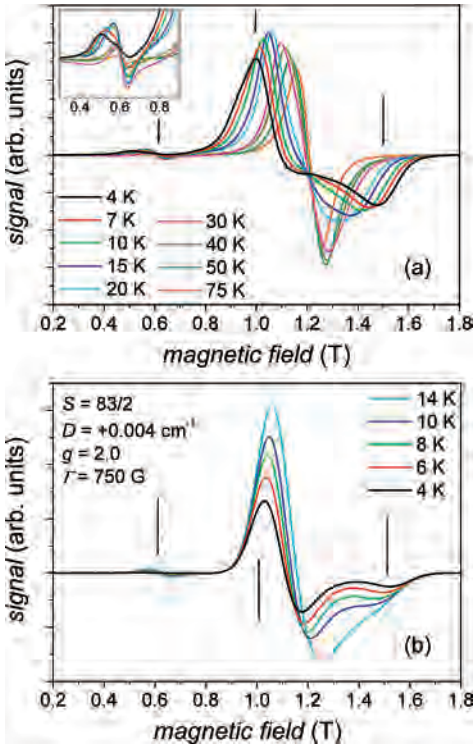

Figure 1. (a) Q-band EPR spectra of a powder sample of Mn_{19} at several temperatures. The arrows indicate features discussed in the text. (b) Simulated Q-band EPR spectra for a zero-field-splitting parameters $D = 0.004$ cm^{-1} at various temperatures ($S = {}^{83}/_{2}$; $g = 2.0$; $\Gamma = 750$ G). The arrows indicate features discussed in the text.

material by fine grinding and one that was prepared by immersing many crystallites in grease. For both samples, the EPR spectra are essentially equivalent, which rules out problems due to insufficient powder averaging, alignment of crystallites in the field, degradation of the sample during grinding, etc. Even a very little amount of sample was found to yield very strong EPR signals, i.e., overloading of the EPR cavity, which required displacement of the sample from the cavity's center; hence, the EPR signal is not perfectly calibrated.

The powder EPR spectra of Mn_{19} at several temperatures are shown in Figure 1a. At 75 K, a typical $g = 2$ EPR signal is seen ($g = 2.008$), which toward lower temperatures spreads out and develops three features at ca. 0.6, 1.0, and 1.5 T. From the temperature dependence, it is clear that the system is not yet in a pure ground state at 4 K, but nearly so. It is noteworthy that the weak 0.6 T feature is strongest at about 15 K (inset to Figure 1a).

The low-temperature EPR data can be well simulated with the simple model of an isolated $S = {}^{83}/_{2}$ spin with uniaxial magnetic anisotropy, $H = DS_z^2 + g\mu_B \mathbf{S}\cdot\mathbf{B}$. Figure 2 presents simulations of the EPR signal at 8 K for a sequence of negative and positive D values (the simulations were done with H. Weihe's program SIM[5]). A survey in the range $D = -0.1$ to $+0.1$ cm^{-1} yielded that D must be smaller in magnitude than 0.01 cm^{-1}. The comparison of the simulations with the experiment shows the following:

(5) Glerup, J.; Weihe, H. *Acta Chim. Scand.* **1991**, *45*, 444.

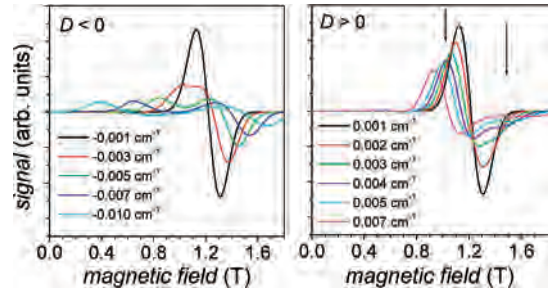

Figure 2. Simulated Q-band EPR spectra at 4 K for various zero-field-splitting parameters $D < 0$ and $D > 0$ ($S = {}^{83}/_{2}$; $g = 2.0$; $\Gamma = 750$ G). The arrows indicate the position of experimentally detected features.

(i) The simulations for negative D are quite at odds with the data. For positive and negative D values, the features in the EPR spectrum do appear at the same field but with a very different pattern of the intensities due to the effects of the temperature. The intensity patterns "very weak", "strongest", and "less strong" for the three features at 0.6, 1.0, and 1.5 T are in accordance only with $D > 0$; hence, D has to be positive.

(ii) The main features at 1.0 and 1.5 T are well reproduced with a D value of about 0.004 cm^{-1}. In contrast, the feature at 0.6 T is not reproduced by the model for $T = 4$ K.

Figure 1b presents simulated EPR spectra for $D = 0.004$ cm^{-1} at several temperatures. Clearly, at elevated temperatures, a weak feature at about 0.6 T develops, which at about 15 K has gained a relative intensity (as compared to the main features at 1.0 and 1.5 T) very similar to that observed. We conclude that in the nominal 4 K experiment the actual sample temperature was significantly higher. For higher temperatures, the simulated spectrum would show a further increase of the 0.6 T feature, at the cost of the central features. This, however, is because in the real material higher lying states are present, which are not included in the model. Indeed, the magnetization curves in ref 4 exhibit a deviation from scaling (if plotted as a function of B/T) for temperatures above about 10 K, confirming this interpretation.

The general behavior of the EPR spectrum is explained as such. For a $S = {}^{83}/_{2}$ multiplet, quite many transitions are allowed by the EPR selection rule $\Delta M = \pm 1$. For instance, for fields along the anisotropy axis z, $2S = 83$ transitions occur [in general, in principle, up to $(2S)!$ transitions are possible]. Because of the small D value, the transitions are very close to each other on the magnetic field axis and not resolved individually; i.e., the EPR spectrum results from the superposition of many transitions. However, the total anisotropy splitting of the $S = {}^{83}/_{2}$ multiplet is $1722D$, or about 6.9 cm^{-1} = 10 K, in zero field. Therefore, the temperature has a pronounced effect, which allows one to clearly distinguish between positive or negative D. For $D > 0$, the states with large M are at the top, and the corresponding transitions (e.g., the $M = {}^{83}/_{2}$ to ${}^{81}/_{2}$ transition) will become significant only at higher temperatures. For $D < 0$, the large-M states are at the bottom and strongest at the lowest temperatures. The feature at 0.6 T is due to large-M transitions, explaining its behavior with temperature in Figure 1.

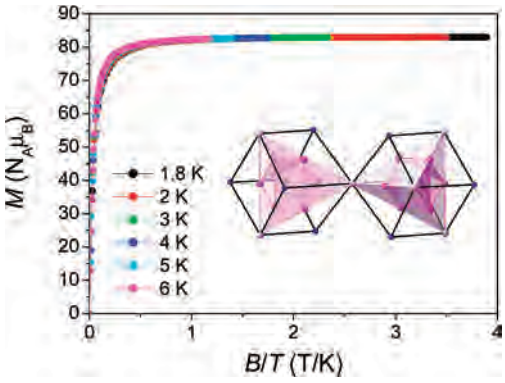

Figure 3. Simulated powder magnetization M vs B/T at the indicated temperatures and fields in the range 0−7 T ($S = {}^{83}/_{2}$; $g = 2.0$; $D = 0.004$ cm^{-1}). Inset: Polyhedral representation of the core of Mn_{19} indicating the two Mn^{III} octahedra discussed in the text (Mn^{III}, dark pink; Mn^{II}, pale pink; N, blue).

In summary, the assumed model reproduces well all observed characteristics in the EPR spectrum. The three features at 0.6, 1.0, and 1.5 T are obtained correctly with regards to both the field positions and the intensity pattern; also the temperature dependence is consistent with experiment.

However, some differences in the details should be noted. The experimental and simulated EPR spectra in the field range 1.1−1.5 T show an opposite trend of their intensities. Also, the 0.6 T feature shows indications of inhomogeneous broadening. These observations could be due to several effects: further anisotropy terms in the spin Hamiltonian, anisotropic line widths, distortion of the lines because of the strong absorption, D strain in the sample, etc.

The total anisotropy splitting of the $S = {}^{83}/_{2}$ multiplet of about 10 K is not negligible as compared to 6 K, up to which scaling of the magnetization curve was observed.[4] However, a D value of 0.004 cm^{-1} is consistent with the observation of scaling, as demonstrated in Figure 3, which shows simulated powder magnetization curves (for $D = 0.004$ cm^{-1}, deviations from scaling occur but are very small; for $|D| >$ 0.02 cm^{-1}, however, the deviations would become significant and would be clearly detected).

In conclusion, we find that the powder EPR spectrum of Mn_{19} at low temperatures is well described by the model of an isolated spin of $S = {}^{83}/_{2}$ with $D = 0.004$ cm^{-1}. The anisotropy is of the hard-axis type; hence, Mn_{19} is not a SMM. The magnetic hysteresis observed below 0.5 K in the previous experiments[4] should be attributed to intermolecular dipole interactions.

As a result of their Jahn−Teller distortions, Mn^{III} ions usually exhibit significant easy-axis anisotropies in the order of several reciprocal centimeters.[6] If one assumes that all Mn^{III} ions in Mn_{19} contribute equally and that the anisotropy of the Mn^{II} ions is negligible, then the local anisotropy of a single Mn^{III} ion is estimated to be $D_{Mn^{III}} \approx 0.2$ cm^{-1},[7] which is an order of magnitude smaller than expected and of the wrong sign. This would suggest that the Mn^{III} anisotropy tensors are tilted away from the cluster anisotropy axis (C_3 axis) with an angle close to but slightly larger than the magic angle. Alternatively, in view of the fact that the six Mn^{III} ions in each "half" of Mn_{19} (inset to Figure 3) form virtually perfect octahedra and that, as previously pointed out in ref 4, the anisotropy tensors of the Mn^{III} ions are arranged to almost perfectly compensate for each other, we can suggest that the cluster anisotropy arises only from the Mn^{II} ions. Then one estimates $D_{Mn^{II}} \approx 0.2$ cm^{-1},[7] which is on the right order of magnitude.[6] In any case, the small observed D value is obviously due to an unfortunate, from the SMM point of view, cancelation of the local anisotropies in Mn_{19}. However, this implies that an even small twisting of the structure by chemical variation may have a large effect on the cluster magnetic anisotropy and potentially results in a negative D value and SMM behavior.

Acknowledgment. Financial support by EC-RTN-QUEMOLNA (Contract No. MRTN-CT-2003-504880) and the DFG Center for Functional Nanostructures is acknowledged.

IC800213W

(6) Boca, R. *Coord. Chem. Rev.* **2004**, *248*, 757.

(7) In the strong-exchange limit, which is consistent with our EPR findings, the cluster anisotropy tensor **D** is connected to the local Mn anisotropy tensors $\mathbf{D}_i$ according to $\mathbf{D} = \sum d_i \mathbf{D}_i$, where $d_i = S_i(2S_i - 1)/[S(2S - 1)]$ are the projections in the ferromagnetic state. If all Mn^{III} ions with $S_i = 2$ contribute equally to the cluster anisotropy and the contributions of the Mn^{II} ions are negligible, then this implies the relation $D = 12 \times 6/3403\ D_{Mn^{III}}$. If, on the other hand, the anisotropy tensors $\mathbf{D}_i$ of the Mn^{III} ions are identical in magnitude but oriented such that they cancel exactly to zero, then only the anisotropies of the Mn^{II} ions with $S_i = {}^{5}/_{2}$ contribute, implying the relation $D = 7 \times 10/3403\ D_{Mn^{II}}$.